TISSUE ENGINEERING: Part A
Volume 19, Numbers 21 and 22, 2013

DOI: 10.1089/ten.tea.2013.0024

Fibronectin Matrix Mimetics Promote Full-Thickness Wound Repair in Diabetic Mice

Daniel C. Roy, PhD,[1] Nancie A. Mooney, MS,[1] Carol H. Raeman, AAS,[1]
Diane Dalecki, PhD,[1] and Denise C. Hocking, PhD[1,2]

During tissue repair, fibronectin is converted from a soluble, inactive form into biologically active extracellular matrix (ECM) fibrils through a cell-dependent process. ECM fibronectin promotes numerous cell processes that are critical to tissue repair and regulates the assembly of other proteins into the matrix. Nonhealing wounds show reduced levels of ECM fibronectin. To functionally mimic ECM fibronectin, a series of fibronectin matrix mimetics was developed by directly coupling the matricryptic, heparin-binding fragment of the first type III repeat of fibronectin (FNIII1H) to various sequences from the integrin-binding domain (FNIII8–10). The recombinant proteins were produced as glutathione-S-transferase (GST)-tagged fusion proteins for ease of production and purification. Full-thickness, excisional wounds were produced in genetically diabetic mice, and fibronectin matrix mimetics were applied directly to the wounds. A significant enhancement of wound closure was observed by day 9 in response to GST/III1H,8–10 versus GST-treated controls (73.9% ± 4.1% vs. 58.1% ± 4.7% closure, respectively). Two weeks after injury, fibronectin matrix mimetic-treated wounds had developed a multi-layered epithelium that completely covered the wound space. Furthermore, significant increases in granulation tissue thickness were observed in response to treatment with GST/III1H,8–10 (4.05 ± 0.93-fold), GST/III1H,8,10 (2.91 ± 0.49-fold), or GST/III1H,8^{RGD} (3.55 ± 0.59-fold) compared with GST controls, and was accompanied by dense collagen deposition, the presence of myofibroblasts, and functional vasculature. Thus, the recombinant fibronectin matrix analogs normalized the impairment in repair observed in this chronic wound model and may provide a new approach to accelerate the healing of diabetic wounds.

Introduction

Cutaneous wound healing is a tightly coordinated, stepwise process that is governed by interactions between cells and the surrounding extracellular matrix (ECM).[1] After injury, inflammatory cells and fibroblasts migrate to the wound space through a provisional matrix that is composed primarily of fibronectin and fibrin.[1] Fibroblasts proliferate within the wound space and synthesize ECM proteins to form the granulation tissue and replace the provisional matrix.[1] This fibronectin- and collagen-rich granulation tissue supports angiogenesis,[2,3] and serves as a scaffold over which epithelial cells migrate from the wound edge inward to resurface the wound and form an intact epidermis.[1,4] During granulation tissue deposition, fibroblasts differentiate into actin-rich myofibroblasts,[5] which, in turn, contract and organize the newly deposited ECM into a compact network.[6,7] Many factors can disrupt the healing process, including infection, diabetes, advanced age, and renal disease, leading to nonhealing, chronic wounds.[1]

Fibronectin matrix assembly is normally up-regulated in response to tissue injury, while decreased fibronectin is associated with nonhealing wounds.[8] Soluble fibronectin is converted into insoluble fibrils in the ECM by a cell-dependent process.[9] The ECM form of fibronectin promotes cell behaviors that are critical to timely wound repair, including myofibroblast growth,[10] epithelial cell migration,[11] and myofibroblast contractility.[12] Fibronectin matrix assembly promotes collagen deposition[13,14] and organization,[12] and increases the tensile mechanical properties of collagen gels.[15] In turn, fibronectin matrix assembly supports endothelial neovessel formation in collagen lattices,[16] promotes vasodilation *in vivo*,[17] and stimulates cellular self-assembly.[18] Thus, the ability of cells to assemble soluble fibronectin into insoluble, bioactive fibrils is likely an important step for efficient wound repair.

The biological activity of ECM fibronectin has been localized, in part, to a matricryptic heparin-binding site in the first type III repeat of fibronectin (FNIII1).[19,20] Buried in soluble fibronectin,[19,21,22] this matricryptic site becomes exposed during the matrix assembly process or as a result of

[1]Department of Biomedical Engineering, University of Rochester, Rochester, New York.
[2]Department of Pharmacology and Physiology, University of Rochester School of Medicine and Dentistry, Rochester, New York.

tension exerted on fibronectin fibrils.[17,23] To deliver ECM fibronectin signals directly to cells, recombinant fibronectin matrix mimetics were engineered by coupling the "open" conformation of FNIII1 (FNIII1H) to variants of the integrin-binding domain (FNIII8–10).[19,24] By design, these fibronectin matrix analogs bypass the requirement for soluble fibronectin to undergo conformational changes in order to initiate ECM fibronectin-specific signals. We previously showed that the fibronectin matrix mimetics GST/III1H,8–10, GST/III1H,8,10, and GST/III1H,8^{RGD} enhance cell growth, migration, and contractility to a similar or greater extent than full-length fibronectin.[24] Fibronectin matrix mimetics stimulate these cell functions through an FNIII1H-dependent mechanism, while specific modifications to the integrin-binding domain enable selective engagement of different integrin receptors.[25] Cell adhesion to GST/III1H,8–10, which contains the complete cell-binding domain,[26] is mediated by α5β1 integrins.[25] Removing FNIII9 (GST/III1H,8,10) results in cell adhesion via both α5β1 and αvβ3 integrins.[25] Deleting FNIII10 and inserting the GRGDSP loop into FNIII8 (GST/III1H,8^{RGD}) results in cell adhesion that is mediated exclusively by αvβ3 integrins.[25] ECM fibronectin, as well as α5β1 and αvβ3 integrins have been implicated as key mediators of cutaneous wound healing.[3,27–29] In the present study, we evaluated the ability of the various fibronectin matrix mimetics to accelerate healing of full-thickness skin wounds in a mouse model of diabetes mellitus type I.

Materials and Methods

Recombinant proteins, reagents, and antibodies

The recombinant proteins, GST/III1H,8–10, GST/III1H,8,10, GST/III1H,8^{RGD}, and GST were produced in *Escherichia coli* and purified as described.[19,24] Hematoxylin and eosin (H&E) were from Leica Microsystems; fibronectin polyclonal and α-tubulin monoclonal (clone DM1A) antibodies were from Sigma; horseradish peroxidase (HRP) goat anti-rabbit and goat anti-mouse antibodies were from Bio-Rad; α-smooth muscle actin (α-SMA) monoclonal antibody (clone 1A4) was from Dako; and mouse-on-mouse HRP-Polymer bundle for monoclonal antibody visualization was from Biocare Medical.

Animals

Male C57BLKS/J (22–28 g) and C57BLKS/J-m+/+Lepr(db) mice (32–51 g) (The Jackson Laboratories) between ages 10 and 16 weeks were used. Mice were housed one per cage and maintained in a central animal care facility. Water and laboratory chow were supplied *ad libitum*. Glucose levels were measured weekly using a TRUEtrack® Blood Glucose Monitoring System (Nipro Diagnostics) (Supplementary Table S1A; Supplementary Data are available online at www.liebertpub.com/tea). Blood was obtained from the tail vein of anesthetized mice. Mice with glucose levels greater than 300 mg/dL were considered diabetic,[30] and mice exhibiting glucose levels less than 300 mg/dL were excluded from the studies. Mice were weighed daily using an MXX-612 Balance (Denver Instrument) to monitor health status (Supplementary Table S1B). All experimental animal procedures were reviewed and approved by the University Committee on Animal Resources at the University of Rochester Medical Center.

Animal surgery

Three days before surgery, mice were administered acetaminophen (Mapap) at a final concentration of 0.5 mg/mL in water, to achieve a therapeutic dose of ~250 mg/kg, based on water consumption. Mice were anesthetized using a combination of ketamine (120 mg/kg; Hospira) and xylazine (9.6 mg/kg; VEDCO); buprenorphine (0.1 mg/kg) was administered to the mice immediately before surgery. An area on the dorsal flank was shaved, and Nair® was applied to remove all hair. Nair application did not result in any noticeable irritation. The flank was cleaned thoroughly with water, followed by iodide and 70% ethanol. Full-thickness skin wounds were made on the dorsal flank using a sterile 6 mm biopsy punch (Miltex). Animals were given 1 mL of subcutaneous saline in the scruff of the neck after surgery. Mice continued to receive water that contained acetaminophen until day 5 postsurgery, at which point acetaminophen was removed.

Recombinant proteins were filter sterilized and suspended in phosphate-buffered saline (PBS) at a final concentration of 25 μM. A 15-μL volume of recombinant protein or PBS alone was pipetted directly onto the wound, and the wounds were immediately sealed from the environment with Tegaderm (3M Health Care). Diabetic mice were anesthetized and treated with proteins on days 2, 4, 7, 9, and 11 after surgery. New Tegaderm was applied after each treatment.

Wound closure

Images of the wounds were obtained immediately after surgery and on treatment days, using a Kodak Gel Logic 112 Imaging System and Carestream software (Kodak). Images were obtained after removal of the Tegaderm dressing. Wounds were traced using Carestream software to determine wound area. Wound closure was measured by tracing the leading edge of epithelium within the wound. Wounds were considered closed if the moist granulation tissue or fascia appeared covered with epithelium.[31] The wound area immediately after surgery (Day 0) was referred to as the original wound area, and all subsequent wound areas were recorded as a percentage of the original area, as previously described.[32–34] Wound closure is presented as "Percent Closure" and was determined as follows:

Percent Closure = [1 − (Wound Area (from leading edge of epithelium)/Original Wound Area)] × 100

Wound contraction was also determined from corresponding images by tracing the area bordered by the original wound edge,[31,35] which could be clearly distinguished from the leading edge of the new epithelium. Wound contraction is presented as "Percent Contraction" and was determined by comparing the area of the wound bordered by the original wound edge to the area of the wound on day 0 as follows:

Percent Contraction = [1 − (Wound Area (from original wound border)/Original Wound Area)] × 100

Fibronectin quantification

Full-thickness skin sections (between 120 and 400 mg) were removed from the dorsal flank of either wild type or diabetic mice. The tissue section was minced with a scalpel, frozen on dry ice, and suspended at 50 mg/mL in 1% deoxycholate (DOC) buffer.[36–38] The tissue was pulverized using a Dounce homogenizer (Wheaton) and incubated for

3 h at 4°C.[38] Samples were then centrifuged for 35 min at 35,000*g* at 4°C to separate DOC-insoluble and DOC-soluble fractions.[38] Aliquots (50 μL) were removed from both the DOC-insoluble and DOC-soluble fractions, treated with reducing sodium dodecyl sulfate (SDS) sample buffer,[39] and analyzed by SDS-polyacrylamide gel electrophoresis (PAGE) and immunoblotting using enhanced chemiluminescence (Thermo Fisher Scientific).[12] Immunoblot band intensity was quantified using Carestream software. DOC-insoluble fibronectin values were normalized using the corresponding α-tubulin band intensities.

Histological analysis

Histological sections were obtained from randomly chosen animals. Seven, 11, or 14 days after wounding, animals were sacrificed and 1 × 1 cm sections of skin surrounding the wound were excised down to the fascia, fixed in 10% formalin, and embedded in paraffin. Five-micrometer sections were cut sequentially through the 1 × 1-cm skin samples to capture the entire wound space. Four sections were mounted on a slide, and every 20th slide was stained with H&E to identify the center of the wound. Unstained slides nearest the center of the wound were processed with Masson's trichrome stain or incubated with antibodies directed against α-SMA. Slides were viewed using an inverted microscope (Olympus IX70). Overlapping images of the wound space were obtained with a digital camera (MicroPublisher 3.3; QImaging) and reconstructed using Photoshop (Adobe).

Quantifying re-epithelialization

Tissue sections corresponding to the center of the wound were used to measure re-epithelialization on day 7, independent of wound contraction. Masson's trichrome stain was used to clearly distinguish between dermis, epithelium, and the panniculus carnosus. The entire length of the epidermal-dermal junction from the edge of the panniculus carnosus to the leading edge of the epithelium was traced using ImageJ.[40] Traces were quantified for both the left and right sides of the wound, then summed to give the total distance migrated.

Quantifying granulation tissue deposition

Granulation tissue thickness was measured on day 14 using H&E stained sections obtained from the center of the wound. Granulation tissue thickness was defined as the distance of intact tissue from the bottom of the epidermis to the top of the subcutaneous fat layer and was quantified using ImageJ.

Statistical analysis

Data are presented as mean ± standard error of the mean (SEM) and are compiled from at least four separate animals per treatment condition that underwent surgical procedures on separate days. Statistical comparisons were performed using either a Student's unpaired *t*-test or a one-way analysis of variance (ANOVA) followed by the Bonferroni post-test, with

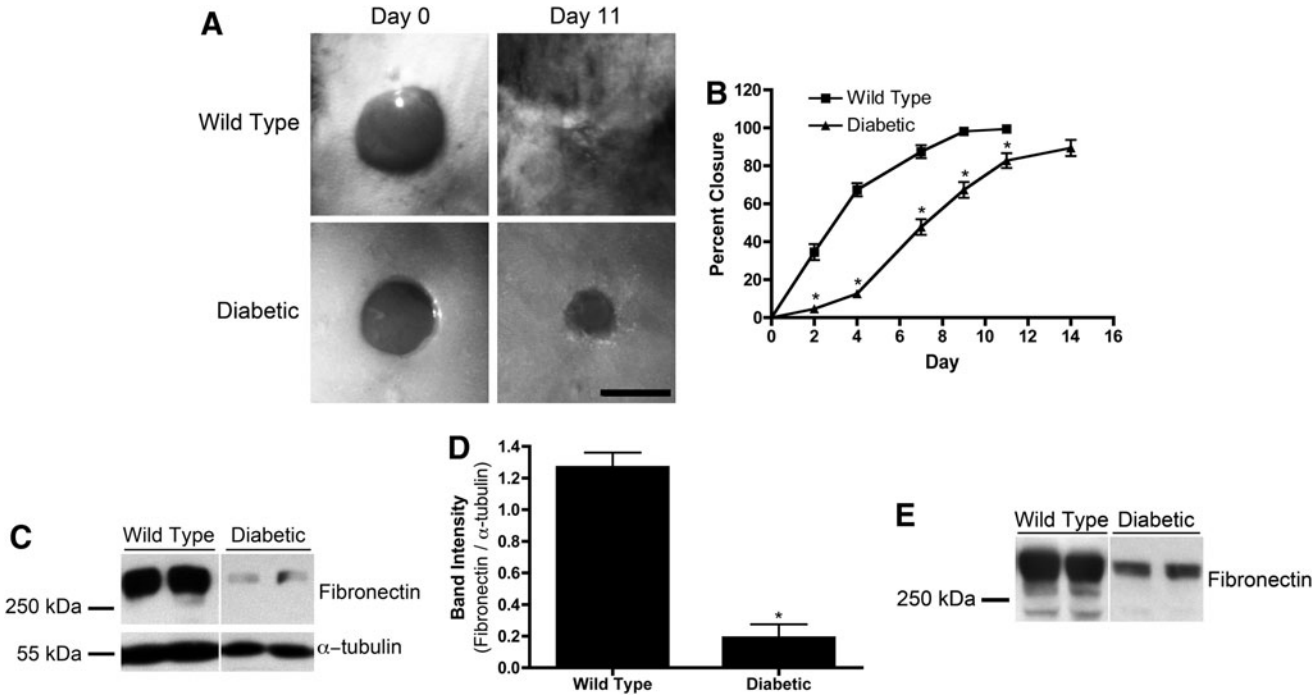

FIG. 1. Wound closure and extracellular matrix fibronectin. **(A, B)** Full-thickness skin wounds were made on wild-type ($n=8$) or diabetic ($n=6$) mice. **(A)** Representative images of wounds immediately after surgery ("Day 0") and on day 11. Scale bar = 5 mm. **(B)** Percent closure is reported as mean percent closure ± standard error of the mean (SEM). *Significantly different from "Wild Type", $p<0.05$ analysis of variance (ANOVA). **(C–E)** Skin samples of uninjured wild-type ($n=8$) and diabetic ($n=6$) mice were extracted with deoxycholate (DOC) detergent. Representative immunoblots of 50 μL of reduced DOC-insoluble **(C)** and corresponding DOC-soluble **(E)** fractions of four mice are shown. **(D)** Fibronectin band intensities of DOC-insoluble fractions were quantified and normalized with α-tubulin. Data represent mean band intensity ratio ± SEM. *Significantly different from "Wild Type", $p<0.05$ (unpaired *t*-test).

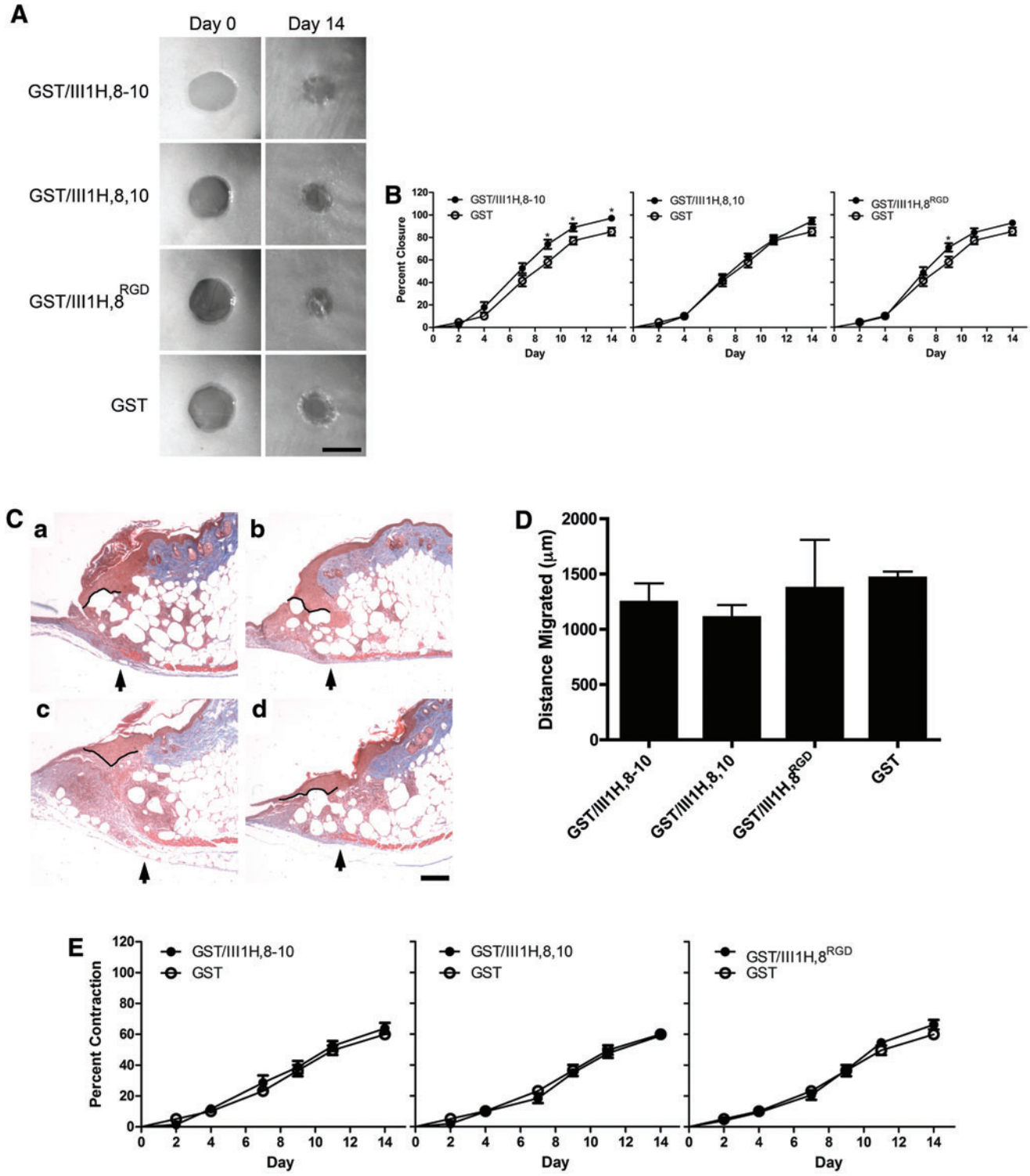

FIG. 2. Fibronectin matrix mimetics accelerate closure of diabetic wounds. Full-thickness wounds on diabetic mice were treated with 25 μM **(a)** glutathione-S-transferase (GST)/III1H,8–10 ($n=12$), **(b)** GST/III1H,8,10 ($n=14$), **(c)** GST/III1H,8^{RGD} ($n=13$), or **(d)** GST ($n=13$). **(A)** Representative images of wounds immediately after surgery ("Day 0") and on day 14. Scale bar = 5 mm. **(B)** Percent closure over time was determined. Data are presented as mean value ± SEM. *Significantly different from GST, $p<0.05$ (ANOVA). **(C)** Representative images of the edge of the wound on day 7, processed with Masson's trichrome stain. Arrows indicate the edge of the panniculus carnosus. Black lines indicate re-epithelialization along the epidermal–dermal junction. Scale bar = 200 μm. **(D)** Re-epithelialization on day 7 reported as mean distance ± SEM for four mice per treatment. **(E)** Wound contraction over time was determined. Data are presented as mean value ± SEM. No significant differences were observed among treatments (ANOVA). Color images available online at www.liebertpub.com/tea

GraphPad Prism Version 4 software. Differences were considered significant for p-values less than 0.05.

Results

Diabetic mice display reduced healing and decreased cutaneous ECM fibronectin

C57BLKS/J-m+/+Lepr(db), genetically diabetic mice are a model for chronic wounds, due in part to their reduced healing ability compared with wild-type, nondiabetic mice.[41] Full-thickness, 6 mm-diameter punch biopsy wounds were made on the dorsal flank of wild-type and genetically diabetic mice. Wounds were imaged over the course of 2 weeks, and the areas of the wounds were determined. Shown in Figure 1A are representative images of wounds on days 0 and 11 of nondiabetic and diabetic mice. Wounds of nondiabetic mice were 98.1%±0.4% closed by day 9 (Fig. 1B). Diabetic wounds were significantly less closed compared with nondiabetic mice on days 2, 4, 7, 9, and 11 and achieved only 89.4%±4.3% closure by day 14 (Fig. 1B).

The amount of ECM fibronectin present in uninjured diabetic mouse skin was quantified and compared with nondiabetic mouse skin. Detergent extractions were performed on full-thickness skin sections to separate soluble fibronectin from insoluble, ECM fibronectin.[36] The amount of fibronectin contained in each fraction was quantified by immunoblot analysis. Wild-type, nondiabetic mouse skin contained significantly more ECM fibronectin than diabetic mouse skin (Fig. 1C). When normalized to α-tubulin, nondiabetic mouse skin contained approximately sevenfold more ECM fibronectin compared with diabetic mouse skin (Fig. 1D). Similarly, nondiabetic mouse skin contained 2.56±0.18-fold more soluble fibronectin than diabetic mouse skin (Fig. 1E; $p<0.05$ by unpaired t-test). Thus, the skin of diabetic mice contains significantly less fibronectin, in both soluble and ECM forms, than the skin of nondiabetic mice.

Fibronectin matrix mimetics accelerate wound closure of diabetic mice

We next tested whether topical application of recombinant fibronectin matrix mimetics to diabetic wounds would accelerate wound closure. Full-thickness skin wounds in diabetic mice were treated topically with GST/III1H,8–10, GST/III1H,8,10, GST/III1H,8^{RGD}, or GST and wound closure, as denoted by the leading edge of the epithelium, was measured over the course of 2 weeks. Representative images of wounds immediately after surgery ("Day 0") and on day 14 after wounding are shown in Figure 2A. No difference in closure rate was observed between wounds treated with the control protein, GST, and the vehicle control, PBS (not shown). Application of GST/III1H,8–10 to wounds significantly accelerated closure compared with GST treatment on days 9 (73.9%±4.1% vs. 58.1%±4.7%), 11 (88.9%±3.6% vs. 77.1%±3.3%), and 14 (97.2%±2.8% vs. 85.2%±3.5%) postwounding (Fig. 2B). Further, wounds treated with GST/III1H,8–10 exceeded 85% closure 3 days earlier than GST-treated wounds (Fig. 2B; compare GST/III1H,8–10, day 11 with GST, day 14). Application of GST/III1H,8,10 to wounds did not accelerate wound closure compared with GST (Fig. 2B). Application of GST/III1H,8^{RGD} to wounds increased closure over GST on day 9 (71.0%±3.7% vs. 59.2%±4.5%; Fig. 2B).

Histological sections of day 7 wounds were also evaluated for differences in re-epithelialization in order to assess wound closure at an earlier time point. For these studies, the panniculus carnosus was used to identify the edges of the original wound.[40] Re-epithelialization was then determined by tracing the epidermal–dermal junction from the edge of the panniculus carnosus (Fig. 2C, arrows) to the leading edge of the epithelium. Fibronectin matrix mimetic treatment did not increase epithelial migration by day 7 compared with GST controls (Fig. 2D).

Wound contraction was also determined over the 2-week period by comparing the area of the wound bordered by the

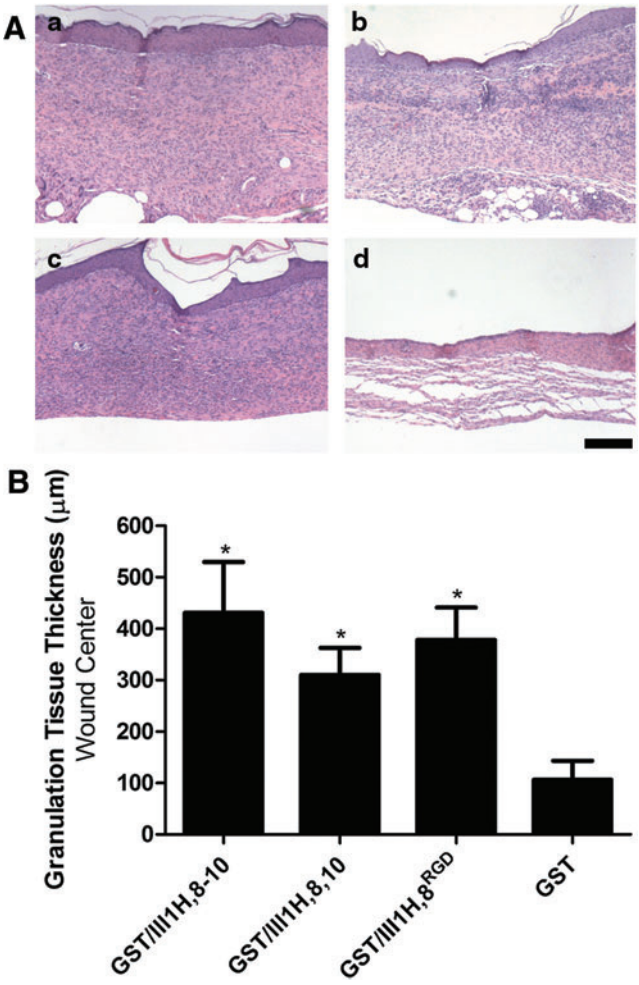

FIG. 3. Fibronectin matrix mimetics increase granulation tissue deposition. Full-thickness skin wounds on the dorsal flank of diabetic mice were treated with 25 μM **(a)** GST/III1H,8–10 ($n=7$), **(b)** GST/III1H,8,10 ($n=9$), **(c)** GST/III1H,8^{RGD} ($n=9$), or **(d)** GST ($n=8$) as described in Materials and Methods section. Fourteen days after surgery, animals were sacrificed, the skin surrounding the wound was excised, and sections were processed for hematoxylin and eosin (H&E). **(A)** Sections from the center of the wound stained with hematoxylin and eosin. Scale bar = 200 μm. **(B)** Granulation tissue thickness was quantified at the center of the wound for each mouse as described in Materials and Methods section. Data are presented as the mean granulation tissue thickness±SEM. *Significantly different from GST, $p<0.05$ (ANOVA). Color images available online at www.liebertpub.com/tea

original wound edge to the area of the wound on day 0.[31,35] On day 14, diabetic wounds had contracted to ~40% of their original area (Fig. 2E). However, no difference in wound contraction between fibronectin matrix mimetic-treated wounds and GST-treated control wounds was observed (Fig. 2E).

Fibronectin matrix mimetics increase granulation tissue deposition

Granulation tissue deposition at the center of the wound was quantified 14 days after wounding to assess healing independent of re-epithelialization. Granulation tissue deposition was quantified by measuring the thickness of the granulation tissue at the center of the wound, from the epidermis to the subcutaneous fat layer. A significant increase in granulation tissue thickness was observed in response to treatment with GST/III1H,8–10 (4.05 ± 0.93-fold), GST/III1H,8,10 (2.91 ± 0.49-fold), or GST/III1H,8^{RGD} (3.55 ± 0.59-fold) compared with GST controls (Fig. 3A, B). For a comparison, the average granulation tissue thickness of day 11, fully closed wounds from wild-type mice was 775.2 ± 71.75 μm ($n = 4$), which was significantly greater than that of day 14 diabetic wounds treated with the fibronectin matrix mimetics ($p > 0.05$, by ANOVA).

Granulation tissue composition of nondiabetic wounds

During normal healing, the fibronectin- and collagen-rich granulation tissue is replaced by a predominantly collagenous matrix.[42] The collagen matrix is subsequently contracted into a tightly woven network by myofibroblasts.[1,7] To determine the composition of the wound space under normal healing conditions, a histological analysis was performed on sections taken from wounds of wild-type, nondiabetic mice 11 days after wounding. As expected,[43] granulation tissue in wounds of nondiabetic mice contained less collagen than the adjacent, uninjured tissue (Fig. 4a, b). Uninjured skin from diabetic mice was composed of a thin layer of dense collagen on top of a layer of fatty tissue (Fig. 4c).

Fibroblasts differentiate into actin-rich myofibroblasts during the remodeling phase of wound healing.[5,7] Antibodies directed against α-SMA were used to identify myofibroblasts within the wound and in the surrounding uninjured tissue. Uninjured skin from both nondiabetic and diabetic mice lacked α – smooth muscle actin stain (Fig. 4d, f). As expected,[7] α-SMA was present in the center of normal wounds in nondiabetic mice 11 days after injury (Fig. 4e).

Collagen deposition and α-SMA staining of diabetic wounds

Collagen deposition and the presence of α-SMA staining within the center of the wound space of diabetic mice were assessed 14 days after injury. Diabetic wounds treated with GST/III1H,8–10 (Fig. 5A, a), GST/III1H,8,10 (Fig. 5A, b), or GST/III1H,8^{RGD} (Fig. 5A, c) contained dense, collagen-rich granulation tissue that spanned the entire wound space. In contrast, GST-treated control wounds contained a thin layer of granulation tissue with limited collagen deposition, particularly toward the center of the wound (Fig. 5A, d).

α-SMA stain was visible at the wound edges and within the center of the granulation tissue of fibronectin matrix mimetic-treated wounds (Fig. 5B). High-magnification images confirmed that widespread α-SMA staining was present at the edge of diabetic wounds in all treatment conditions (Fig. 5C, "Edge"). Wounds treated with GST/III1H,8–10 (Fig. 5C, a), GST/III1H,8,10 (Fig. 5C, b), and GST/III1H,8^{RGD} (Fig. 5C, c) exhibited α-SMA stain within the center of the granulation tissue, indicating cellular infiltration into the wound bed. In contrast, α-SMA staining was not visible within the center of the GST-treated wound by day 14 (Fig. 5C, d). Together, these data indicate that application of fibronectin matrix mimetics to diabetic wounds promotes a uniform deposition of collagen-rich granulation tissue that supports increased cellularity across the entire width of the wound bed.

Revascularization of diabetic wounds

Granulation tissue serves as a scaffold for angiogenesis during wound repair.[1,2] In turn, blood vessels supply the wound space with nutrients and oxygen to support sustained healing.[43] To determine whether vasculature is present in the granulation tissue of wounds treated with the fibronectin matrix mimetics, high-magnification images were obtained from the center of the wound space. Masson's trichrome stain

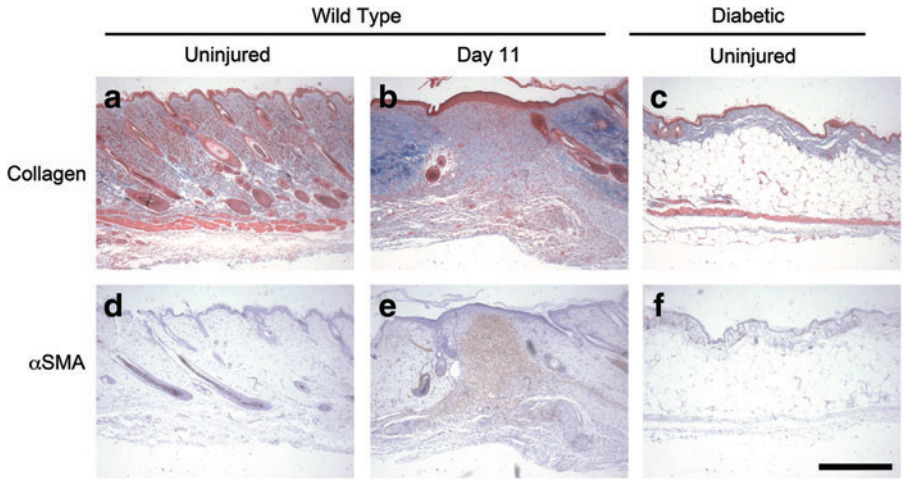

FIG. 4. Histological analysis of nondiabetic wounds. Full-thickness skin wounds were made on the dorsal flank of wild-type mice. Eleven days after wounding, animals were sacrificed and the skin surrounding the wound site was excised and processed for histological analysis. Skin sections were obtained away from the wound ("Uninjured") and through the center of the wound site ("Day 11"). Uninjured skin from diabetic mice was also processed for histological analysis. Sections were stained using either Masson's trichrome **(a–c)** or antibodies directed against α-smooth muscle actin (α-SMA) **(d–f)**. Scale bar = 500 μm. Color images available online at www.liebertpub.com/tea

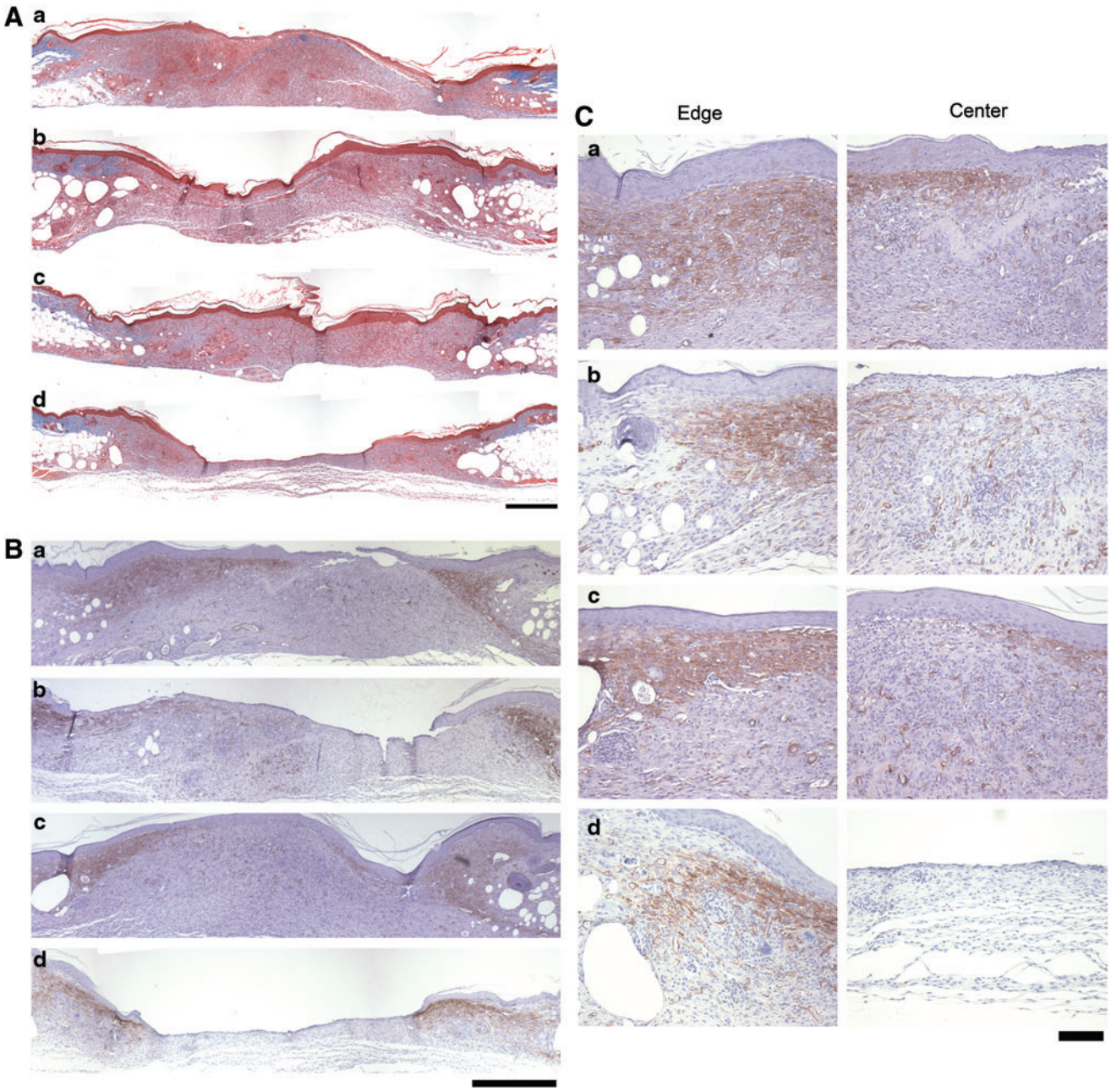

FIG. 5. Collagen and smooth muscle actin staining of diabetic wounds after treatment with fibronectin matrix mimetics. Full-thickness skin wounds were made on the dorsal flank of diabetic mice. Wounds were treated with 15 μL of 25-μM **(a)** GST/III1H,8–10 ($n=7$), **(b)** GST/III1H,8,10 ($n=9$), **(c)** GST/III1H,8^{RGD} ($n=9$), or **(d)** GST ($n=8$) immediately after surgery and on days 2, 4, 7, 9, and 11 postsurgery. Fourteen days after surgery, animals were sacrificed, and the skin surrounding the wound was excised and processed for **(A)** Masson's trichrome stain or **(B, C)** stained using an α-SMA monoclonal antibody (brown). Representative images were obtained at the edge and center of the wound. **(A, B)** Scale bar = 500 μm. **(C)** Scale bar = 100 μm. Color images available online at www.liebertpub.com/tea

was used to identify red blood cells; antibodies directed against α-SMA were used to visualize pericytes and vascular smooth muscle cells in blood vessel walls.[44] Granulation tissue of wounds treated with GST/III1H,8–10 (Fig. 6a, b), GST/III1H,8,10 (Fig. 6c, d), and GST/III1H,8^{RGD} (Fig. 6e, f) showed functional, erythrocyte-containing blood vessels within the center of the wound space. These data indicate that the granulation tissue deposited by fibronectin matrix mimetic-treated wounds supports vascularization.

Discussion

In this study, we report that topical application of recombinant fibronectin matrix mimetics to full-thickness excisional wounds in diabetic mice accelerates wound closure and promotes granulation tissue formation. Application of GST/III1H,8–10 to diabetic wounds significantly increased the extent of wound closure by day 9 compared with GST-treated controls, and by day 14, the epithelium was multi-layered.

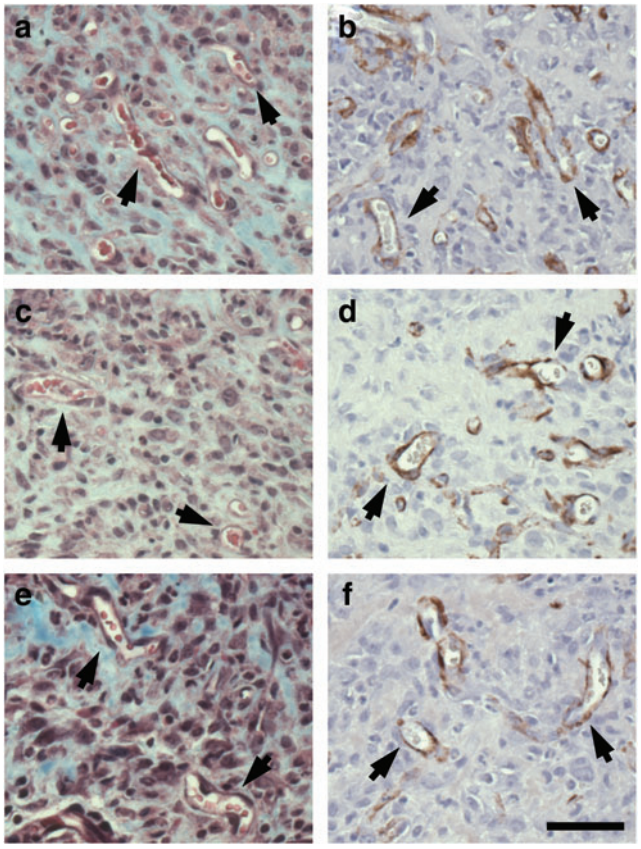

FIG. 6. Revascularization of diabetic wounds. Full-thickness skin wounds were made on the dorsal flank of diabetic mice. Wounds were treated with 15 μL of 25-μM **(a, b)** GST/III1H,8–10 ($n=7$); **(c, d)** GST/III1H,8,10 ($n=9$); or **(e, f)** GST/III1H,8^{RGD} ($n=9$) immediately after surgery and on days 2, 4, 7, 9, and 11 postsurgery. Fourteen days after surgery, animals were sacrificed, and the skin surrounding the wound was excised and processed using either **(a, c, e)** Masson's trichrome stain, or **(b, d, f)** an α-SMA monoclonal antibody (brown). Representative images were obtained at the center of the wound. Arrows indicate blood vessels. Scale bar = 50 μm. Color images available online at www.liebertpub.com/tea

Application of the fibronectin matrix mimetics GST/III1H,8–10, GST/III1H,8,10, or GST/III1H,8^{RGD} significantly increased granulation tissue deposition over GST-treated wounds. Granulation tissue of wounds treated with the fibronectin matrix mimetics was completely covered by epithelium, and characterized by dense collagen throughout the wound space, actin-rich myofibroblasts, and the presence of functional vasculature. These studies provide evidence that fibronectin matrix mimetics, designed to deliver ECM fibronectin-specific signals to cells under conditions where fibronectin matrix assembly is impaired, promote the healing and neovascularization of chronic, cutaneous wounds.

The ability of fibronectin matrix mimetics to improve healing was assessed in a well-established murine model of impaired healing that mirrors many of the clinical findings observed in diabetic patients. C57BLKS/J-m+/+Lepr(db) genetically diabetic mice exhibit obesity and hyperglycemia, and are susceptible to immunodeficiency, peripheral neuropathy, and microvascular lesions.[31,45] Genetically diabetic mice experience delayed wound closure and reduced wound contraction compared with wild-type mice.[31,41] Delayed wound healing in genetically diabetic mice is associated with low collagen content, delayed and disorganized fibroblast infiltration, reduced angiogenesis, chronic inflammation, and low wound strength.[46] Similarly, human diabetic wounds demonstrate decreased levels of cellular infiltration after injury, including impaired fibroblast migration and delayed re-epithelialization.[47] Future investigations are necessary to determine the clinical potential of fibronectin matrix mimetics for treatment of nonhealing ulcers in diabetic patients.

Integrin interactions with the surrounding ECM are critical during normal wound repair. β1 integrin-null keratinocytes display impaired migration during cutaneous wound repair in mice.[48] Similarly, mice expressing β1 integrin-null fibroblasts exhibit delayed wound closure and decreased granulation tissue deposition.[34] Fibronectin fragments with binding specificity toward α5β1 integrins have been studied for their ability to aid in various stages of wound repair. The Pro-His-Ser-Arg-Asn (PHSRN) sequence from FNIII9 contributes to the binding specificity of full-length fibronectin for α5β1 integrins.[49] Peptides containing the PHSRN sequence promoted complete re-epithelialization of 4-mm diameter skin wounds in diabetic mice within 8 days of injury.[41] The fibronectin matrix mimetics used in the present study exhibit different integrin-binding specificities.[25] The construct GST/III1H,8–10 contains the PHSRN sequence and binds to cells via α5β1 integrins.[25] Thus, the ability of this construct to engage α5β1 integrins may account for the increase in re-epithelialization observed in the current study.

Uninjured diabetic mouse skin contained significantly less ECM fibronectin than nondiabetic mouse skin (Fig. 1C), which may contribute to the reduced healing response observed in the diabetic mice. In one previous histological study, sections of uninjured skin from diabetic humans showed increased fibronectin staining compared with skin from healthy individuals.[50] Fibronectin in diabetic humans is subject to advanced glycation end products (AGE) that can affect fibronectin structure and function.[51] AGE-modified fibronectin has reduced ability to support cell adhesion, spreading, and migration,[52,53] and to bind to collagen and heparin.[54] As such, the fibronectin fibrils observed in uninjured human diabetic skin may have reduced function. Fibronectin matrix mimetics promote adhesion, spreading, and migration,[24] suggesting that they may be used to overcome the irregularities in cell adhesion and migration associated with AGE-modified fibronectin from diabetic humans.

Nonhealing, diabetic wounds are increasingly prevalent as the number of diabetic patients climbs.[47] Limited therapies are available that offer reliable, cost-effective treatment. Bioengineered skin substitutes have a high procedural cost and only promote closure on roughly half of the diabetic foot ulcers tested.[55] The use of topical growth factors to accelerate re-epithelialization and increase cell infiltration of chronic wounds has also been tested.[31,32,56] Currently, only recombinant platelet-derived growth factor (PDGF; Regranex®) is FDA approved to treat diabetic ulcers.[57] In the present study, we show that topical application of fibronectin matrix mimetics to diabetic wounds strongly promotes the deposition of a collagen-rich, vascularized granulation tissue by day 14. These results are similar to the reported effects of equimolar PDGF on granulation tissue formation of full-thickness

wounds in diabetic mice.[26] Moreover, application of GST/III1H,8–10 significantly increased wound closure as early as day 9. In contrast, no significant differences in wound closure in response to PDGF treatment were observed until day 21 after injury.[26] Treatment of diabetic mouse wounds with fibronectin fragments engineered to bind both integrins and growth factors has been shown to enhance the wound-healing effects of PDGF and vascular endothelial growth factor.[58] Similarly, full-length fibronectin potentiates effects of erythropoietin treatment on wound healing in diabetic mice.[33] As such, fibronectin matrix mimetics could serve as a supplement to other treatment strategies to enhance healing of chronic wounds. The small size of the recombinant fibronectin proteins facilitates production, decreases potential immunogenicity, and provides increased structure and stability compared with peptides. Thus, fibronectin matrix mimetics make attractive candidates for integration into various delivery vehicles, including fibrin sprays[59] and collagen meshes,[60] to promote healing of chronic diabetic wounds.

Acknowledgments

This study was supported in part by NIH grants R01 GM081513 and R01 EB008996. The authors thank Susan Wilke-Mounts and Loralee McMahon for excellent technical assistance.

Disclosure Statement

No competing financial interests exist.

References

1. Singer, A.J., and Clark, R.A. Cutaneous wound healing. N Engl J Med **341,** 738, 1999.
2. Sottile, J. Regulation of angiogenesis by extracellular matrix. Biochim Biophys Acta **1654,** 13, 2004.
3. Kim, S., Bell, K., Mousa, S.A., and Varner, J.A. Regulation of angiogenesis *in vivo* by ligation of integrin alpha5beta1 with the central cell-binding domain of fibronectin. Am J Pathol **156,** 134, 2000.
4. Juhasz, I., Murphy, G.F., Yan, H.C., Herlyn, M., and Albelda, S.M. Regulation of extracellular matrix proteins and integrin cell substratum adhesion receptors on epithelium during cutaneous human wound healing *in vivo*. Am J Pathol **143,** 1458, 1993.
5. Desmouliere, A., Geinoz, A., Gabbiani, F., and Gabbiani, G. Transforming growth factor-beta 1 induces alpha-smooth muscle actin expression in granulation tissue myofibroblasts and in quiescent and growing cultured fibroblasts. J Cell Biol **122,** 103, 1993.
6. Grinnell, F., and Lamke, C.R. Reorganization of hydrated collagen lattices by human skin fibroblasts. J Cell Sci **66,** 51, 1984.
7. Amadeu, T.P., Coulomb, B., Desmouliere, A., and Costa, A.M. Cutaneous wound healing: myofibroblastic differentiation and *in vitro* models. Int J Low Extrem Wounds **2,** 60, 2003.
8. Herrick, S.E., Sloan, P., McGurk, M., Freak, L., McCollum, C.N., and Ferguson, M.W. Sequential changes in histologic pattern and extracellular matrix deposition during the healing of chronic venous ulcers. Am J Pathol **141,** 1085, 1992.
9. Magnusson, M.K., and Mosher, D.F. Fibronectin: structure, assembly, and cardiovascular implications. Arterioscler Thromb Vasc Biol **18,** 1363, 1998.
10. Sottile, J., Hocking, D.C., and Swiatek, P.J. Fibronectin matrix assembly enhances adhesion-dependent cell growth. J Cell Sci **111,** 2933, 1998.
11. Hocking, D.C., and Chang, C.H. Fibronectin matrix polymerization regulates small airway epithelial cell migration. Am J Physiol Lung Cell Mol Physiol **285,** L169, 2003.
12. Hocking, D.C., Sottile, J., and Langenbach, K.J. Stimulation of integrin-mediated cell contractility by fibronectin polymerization. J Biol Chem **275,** 10673, 2000.
13. Velling, T., Risteli, J., Wennerberg, K., Mosher, D.F., and Johansson, S. Polymerization of type I and III collagens is dependent on fibronectin and enhanced by integrins alpha 11beta 1 and alpha 2beta 1. J Biol Chem **277,** 37377, 2002.
14. Sottile, J., and Hocking, D.C. Fibronectin polymerization regulates the composition and stability of extracellular matrix fibrils and cell-matrix adhesions. Mol Biol Cell **13,** 3546, 2002.
15. Gildner, C.D., Lerner, A.L., and Hocking, D.C. Fibronectin matrix polymerization increases tensile strength of model tissue. Am J Physiol Heart Circ Physiol **287,** H46, 2004.
16. Zhou, X., Rowe, R.G., Hiraoka, N., George, J.P., Wirtz, D., Mosher, D.F., *et al.* Fibronectin fibrillogenesis regulates three-dimensional neovessel formation. Genes Dev **22,** 1231, 2008.
17. Hocking, D.C., Titus, P.A., Sumagin, R., and Sarelius, I.H. Extracellular matrix fibronectin mechanically couples skeletal muscle contraction with local vasodilation. Circ Res **102,** 372, 2008.
18. Sevilla, C.A., Dalecki, D., and Hocking, D.C. Extracellular matrix fibronectin stimulates the self-assembly of microtissues on native collagen gels. Tissue Eng Part A **16,** 3805, 2010.
19. Hocking, D.C., and Kowalski, K. A cryptic fragment from fibronectin's III1 module localizes to lipid rafts and stimulates cell growth and contractility. J Cell Biol **158,** 175, 2002.
20. Gui, L., Wojciechowski, K., Gildner, C.D., Nedelkovska, H., and Hocking, D.C. Identification of the heparin-binding determinants within fibronectin repeat III1: role in cell spreading and growth. J Biol Chem **281,** 34816, 2006.
21. Hocking, D.C., Sottile, J., and McKeown-Longo, P.J. Fibronectin's III-1 module contains a conformation-dependent binding site for the amino-terminal region of fibronectin. J Biol Chem **269,** 19183, 1994.
22. Briknarova, K., Akerman, M.E., Hoyt, D.W., Ruoslahti, E., and Ely, K.R. Anastellin, an FN3 fragment with fibronectin polymerization activity, resembles amyloid fibril precursors. J Mol Biol **332,** 205, 2003.
23. Zhong, C., Chrzanowska-Wodnicka, M., Brown, J., Shaub, A., Belkin, A.M., and Burridge, K. Rho-mediated contractility exposes a cryptic site in fibronectin and induces fibronectin matrix assembly. J Cell Biol **141,** 539, 1998.
24. Roy, D.C., Wilke-Mounts, S.J., and Hocking, D.C. Chimeric fibronectin matrix mimetic as a functional growth- and migration-promoting adhesive substrate. Biomaterials **32,** 2077, 2011.
25. Roy, D.C., and Hocking, D.C. Recombinant fibronectin matrix mimetics specify integrin adhesion and extracellular matrix assembly. Tissue Eng Part A **19,** 558, 2013.
26. Pankov, R., and Yamada, K.M. Fibronectin at a glance. J Cell Sci **115,** 3861, 2002.
27. Tonnesen, M.G., Feng, X., and Clark, R.A. Angiogenesis in wound healing. J Investig Dermatol Symp Proc **5,** 40, 2000.
28. Clark, R.A., Tonnesen, M.G., Gailit, J., and Cheresh, D.A. Transient functional expression of alphaVbeta 3 on vascular cells during wound repair. Am J Pathol **148,** 1407, 1996.

29. Clark, R.A. Fibronectin matrix deposition and fibronectin receptor expression in healing and normal skin. J Invest Dermatol **94,** 128S, 1990.
30. Matarese, G., Sanna, V., Lechler, R.I., Sarvetnick, N., Fontana, S., Zappacosta, S., *et al.* Leptin accelerates autoimmune diabetes in female NOD mice. Diabetes **51,** 1356, 2002.
31. Greenhalgh, D.G., Sprugel, K.H., Murray, M.J., and Ross, R. PDGF and FGF stimulate wound healing in the genetically diabetic mouse. Am J Pathol **136,** 1235, 1990.
32. Brown, R.L., Breeden, M.P., and Greenhalgh, D.G. PDGF and TGF-alpha act synergistically to improve wound healing in the genetically diabetic mouse. J Surg Res **56,** 562, 1994.
33. Hamed, S., Ullmann, Y., Egozi, D., Daod, E., Hellou, E., Ashkar, M., *et al.* Fibronectin potentiates topical erythropoietin-induced wound repair in diabetic mice. J Invest Dermatol **131,** 1365, 2011.
34. Liu, S., Xu, S.W., Blumbach, K., Eastwood, M., Denton, C.P., Eckes, B., *et al.* Expression of integrin beta1 by fibroblasts is required for tissue repair *in vivo*. J Cell Sci **123,** 3674, 2010.
35. Tkalcevic, V.I., Cuzic, S., Parnham, M.J., Pasalic, I., and Brajsa, K. Differential evaluation of excisional non-occluded wound healing in db/db mice. Toxicol Pathol **37,** 183, 2009.
36. McKeown-Longo, P.J., and Mosher, D.F. Binding of plasma fibronectin to cell layers of human skin fibroblasts. J Cell Biol **97,** 466, 1983.
37. Xu, J., Bae, E., Zhang, Q., Annis, D.S., Erickson, H.P., and Mosher, D.F. Display of cell surface sites for fibronectin assembly is modulated by cell adherence to (1)F3 and C-terminal modules of fibronectin. PLoS One **4,** e4113, 2009.
38. Rebres, R.A., McKeown-Longo, P.J., Vincent, P.A., Cho, E., and Saba, T.M. Extracellular matrix incorporation of normal and NEM-alkylated fibronectin: liver and spleen deposition. Am J Physiol **269,** G902, 1995.
39. Sambrook, J., Fritsch, E.F., and Maniatis, T. Molecular Cloning: A Laboratory Manual. Cold Spring Harbor: Cold Spring Harbor Laboratory Press, 1989.
40. Eming, S.A., Werner, S., Bugnon, P., Wickenhauser, C., Siewe, L., Utermohlen, O., *et al.* Accelerated wound closure in mice deficient for interleukin-10. Am J Pathol **170,** 188, 2007.
41. Livant, D.L., Brabec, R.K., Kurachi, K., Allen, D.L., Wu, Y., Haaseth, R., *et al.* The PHSRN sequence induces extracellular matrix invasion and accelerates wound healing in obese diabetic mice. J Clin Invest **105,** 1537, 2000.
42. Kurkinen, M., Vaheri, A., Roberts, P.J., and Stenman, S. Sequential appearance of fibronectin and collagen in experimental granulation tissue. Lab Invest **43,** 47, 1980.
43. Broughton, G., 2nd, Janis, J.E., and Attinger, C.E. Wound healing: an overview. Plast Reconstr Surg **117,** 1e-S, 2006.
44. Hughes, S., and Chan-Ling, T. Characterization of smooth muscle cell and pericyte differentiation in the rat retina *in vivo*. Invest Ophthalmol Vis Sci **45,** 2795, 2004.
45. Coleman, D.L. Diabetes-obesity syndromes in mice. Diabetes **31,** 1, 1982.
46. Altavilla, D., Saitta, A., Cucinotta, D., Galeano, M., Deodato, B., Colonna, M., *et al.* Inhibition of lipid peroxidation restores impaired vascular endothelial growth factor expression and stimulates wound healing and angiogenesis in the genetically diabetic mouse. Diabetes **50,** 667, 2001.
47. Brem, H., and Tomic-Canic, M. Cellular and molecular basis of wound healing in diabetes. J Clin Invest **117,** 1219, 2007.
48. Grose, R., Hutter, C., Bloch, W., Thorey, I., Watt, F.M., Fassler, R., *et al.* A crucial role of beta 1 integrins for keratinocyte migration *in vitro* and during cutaneous wound repair. Development **129,** 2303, 2002.
49. Aota, S., Nomizu, M., and Yamada, K.M. The short amino acid sequence Pro-His-Ser-Arg-Asn in human fibronectin enhances cell-adhesive function. J Biol Chem **269,** 24756, 1994.
50. Leutenegger, M., Birembaut, P., Poynard, J.P., Eschard, J.P., Ricard, Y., Caron, Y., *et al.* Distribution of fibronectin in diabetic skin. Pathol Biol (Paris) **31,** 45, 1983.
51. Duran-Jimenez, B., Dobler, D., Moffatt, S., Rabbani, N., Streuli, C.H., Thornalley, P.J., *et al.* Advanced glycation end products in extracellular matrix proteins contribute to the failure of sensory nerve regeneration in diabetes. Diabetes **58,** 2893, 2009.
52. Bhatwadekar, A.D., Glenn, J.V., Li, G., Curtis, T.M., Gardiner, T.A., and Stitt, A.W. Advanced glycation of fibronectin impairs vascular repair by endothelial progenitor cells: implications for vasodegeneration in diabetic retinopathy. Invest Ophthalmol Vis Sci **49,** 1232, 2008.
53. Murillo, J., Wang, Y., Xu, X., Klebe, R.J., Chen, Z., Zardeneta, G., *et al.* Advanced glycation of type I collagen and fibronectin modifies periodontal cell behavior. J Periodontol **79,** 2190, 2008.
54. Cohen, M.P., and Ku, L. Inhibition of fibronectin binding to matrix components by nonenzymatic glycosylation. Diabetes **33,** 970, 1984.
55. Curran, M.P., and Plosker, G.L. Bilayered bioengineered skin substitute (Apligraf): a review of its use in the treatment of venous leg ulcers and diabetic foot ulcers. BioDrugs **16,** 439, 2002.
56. Uhl, E., Barker, J.H., Bondar, I., Galla, T.J., Leiderer, R., Lehr, H.A., *et al.* Basic fibroblast growth factor accelerates wound healing in chronically ischaemic tissue. Br J Surg **80,** 977, 1993.
57. Murphy, P.S., and Evans, G.R. Advances in wound healing: a review of current wound healing products. Plast Surg Int **2012,** 190436, 2012.
58. Martino, M.M., Tortelli, F., Mochizuki, M., Traub, S., Ben-David, D., Kuhn, G.A., *et al.* Engineering the growth factor microenvironment with fibronectin domains to promote wound and bone tissue healing. Sci Transl Med **3,** 100ra89, 2011.
59. Falanga, V., Iwamoto, S., Chartier, M., Yufit, T., Butmarc, J., Kouttab, N., *et al.* Autologous bone marrow-derived cultured mesenchymal stem cells delivered in a fibrin spray accelerate healing in murine and human cutaneous wounds. Tissue Eng **13,** 1299, 2007.
60. Powell, H.M., Supp, D.M., and Boyce, S.T. Influence of electrospun collagen on wound contraction of engineered skin substitutes. Biomaterials **29,** 834, 2008.

Address correspondence to:
Denise C. Hocking, PhD
Department of Pharmacology and Physiology
University of Rochester
Box 711, 601 Elmwood Ave.
Rochester, NY 14642

E-mail: denise_hocking@urmc.rochester.edu

Received: January 14, 2013
Accepted: June 19, 2013
Online Publication Date: August 12, 2013